Pharmacokinetics of [^{18}F]FETNIM: A Potential Hypoxia Marker for PET

Tove Grönroos, Olli Eskola, Kaisa Lehtiö, Heikki Minn, Päivi Marjamäki, Jörgen Bergman, Merja Haaparanta, Sarita Forsback, and Olof Solin

Medicity Research Laboratory and Radiopharmaceutical Chemistry Laboratory, Turku PET Centre, Turku; and Department of Oncology and Radiotherapy, Turku University Central Hospital, Turku, Finland

^{18}F-labeled fluoroerythronitroimidazole (FETNIM) has been suggested as a marker of tumor hypoxia for use with PET. Our goal was to evaluate the pharmacokinetic properties of [^{18}F]FETNIM in rats and analyze metabolites in human, dog, and rat plasma and urine. Metabolites in liver and tumor homogenates from tumor-bearing rats, as well as the biodistribution of the tracer, were also studied. **Methods:** Radio–thin-layer chromatography and digital autoradiography were used to distinguish metabolites from the parent drug in urine and plasma from 8 patients, 3 dogs, and 18 rats, as well as in liver and tumor homogenates from Sprague-Dawley rats bearing 7,12-dimethylbenzanthracene–induced rat mammary carcinoma. Biodistribution of [^{18}F]FETNIM was also studied in rats at 15, 30, 60, 120, and 240 min after tracer injection. **Results:** Most of the radioactivity in plasma and urine was the unchanged tracer, whereas rat liver homogenates contained almost only metabolites of [^{18}F]FETNIM. None of the species studied showed binding of tracer to plasma proteins. A large variation—3%–70%—in the radioactivity represented by unchanged [^{18}F]FETNIM was found in rat tumor. A negative correlation was found between the percentage of radioactivity represented by unchanged [^{18}F]FETNIM in tumor tissue and tumor uptake (percentage injected dose per gram of tissue) at later times. The highest radioactivity was seen in urine and kidney; the lowest uptake was in fat, cerebellum, and bone matrix. In contrast to matrix, bone marrow had high uptake of ^{18}F. The tumor-to-blood ratio reached a maximum of 1.80 ± 0.64 at 2 h. **Conclusion:** We conclude that [^{18}F]FETNIM shows low peripheral metabolism, little defluorination, and possible metabolic trapping in hypoxic tumor tissue. These suggest a potential use for this tracer in PET studies on hypoxia of cancer patients.

Key Words: [^{18}F]fluoroerythronitroimidazole; hypoxia; metabolism; PET; biodistribution

J Nucl Med 2001; 42:1397–1404

Hypoxia in tumors is believed to be an important cause of local failure of radiotherapy (*1*). Detection and quantification of oxygen levels in human tumors may have a high impact on predicting the outcome of patients treated with radiation and on the utility of hypoxia-specific chemother-apeutic agents. Recent experimental studies have also shown that reduced oxygenation of tumor cells may influence malignant progression through effects on signal transduction pathways and the regulation and transcription of various genes involved in neoplastic growth and metabolism (*2–4*).

A variety of techniques for measuring oxygen in tissues has been developed over the years (*5*). Detection of tumor hypoxia by imaging techniques with radiolabeled 2-nitroimidazoles was proposed by Chapman in 1979 (*6*). The reductive metabolism of these compounds leads to their activation and subsequent formation of covalent bonds with cellular macromolecules under hypoxic conditions. Thus, these compounds tend to accumulate in sites of hypoxia and are therefore rendered suitable for imaging. The first studies indicated selective binding of ^{14}C- or ^{3}H-labeled 2-nitroimidazoles in anoxic tumor cells or regions in spheroid systems with confirmed hypoxia (*7*). Since then, labeled fluoromisonidazole (FMISO) has been evaluated for detecting hypoxia in experimental and human tumors with PET (*8–10*). Several other ^{18}F-labeled nitroimidazole compounds with presumed selectivity for imaging hypoxia with PET have also been synthesized and evaluated during the last 2 decades (*11–15*). Recently, ^{64}Cu-labeled Cu-diacetyl-bis(N^4-methylthiosemicarbazone), a thiosemicarbazone ligand (*16*), was introduced as a hypoxia-specific tracer for PET. Agents suitable for use with standard gamma cameras, such as ^{123}I-labeled iodoazomycin arabinoside (*17–19*) and several ^{99m}Tc-labeled compounds (*20–22*), have also been developed.

The synthesis of 4-[^{18}F]fluoro-2,3-dihydroxy-1-(2′-nitro-1′-imidazolyl)butane (fluoroerythronitroimidazole, or FETNIM), which is a more hydrophilic compound than [^{18}F]FMISO, was first described by Yang et al. in 1995 (*12*). The authors indicated that, at 4 h after injection, tumor-to-blood and tumor-to-muscle ratios in mammary tumor–bearing rats were significantly higher with [^{18}F]FETNIM than with [^{18}F]FMISO. However, no subsequent studies have confirmed these early observations, nor are any data available on the pharmacokinetics of this tracer. Encouraged by the initial findings by Yang et al., we studied the pharmacokinetics and metabolism of [^{18}F]FETNIM in rats and metabolite formation in

plasma of dogs and humans. A 7,12-dimethylbenzanthracene (DMBA)–induced mammary cancer was used to study the time course of [18F]FETNIM uptake in multiple tissues. The tracer uptake and formation of metabolites were then evaluated to clarify the potential of this hydrophilic 2-nitroimidazole tracer for imaging with PET.

MATERIALS AND METHODS

Permissions

Permission for the study was obtained from the ethics committee for experimental animals at Turku University. All dogs were studied with the owners' permission and under the surveillance of a certified veterinarian. The patient studies were part of a clinical trial on imaging hypoxia with [18F]FETNIM, and this clinical trial had been reviewed and approved by the joint ethics committee of Turku University and Turku University Central Hospital. Written informed consent was obtained from each patient.

Synthesis of [18F]FETNIM

[18F]FETNIM was synthesized from 1-(2′-nitro-1′-imidazolyl)-2,3-O-isopropylidene-4-tosyloxybutane. The precursor was prepared as reported by Yang et al. (12). [18F]FETNIM was synthesized from the precursor by nucleophilic displacement of the tosyloxy group with [18F]fluoride (18F−) followed by acidic hydrolysis of the diol-protecting group (Fig. 1). The radiochemical synthesis of [18F]FETNIM was slightly modified from the original method (12) as follows.

18F was obtained through the nuclear reaction 18O(p,n)18F. [18F]F− was produced by bombarding 18O-enriched water (450 μL, >96% enrichment) with 17 MeV protons using a cyclotron. The generated radioactivity was approximately 13 GBq (350 mCi) in a 30-min irradiation. The target water was directed to a borosilicate glass reaction vessel containing Kryptofix 222 (18 mg, 48 μmol; Merck AG, Darmstadt, Germany) and anhydrous potassium carbonate (5 mg, 36 μmol). Azeotropic distillation with acetonitrile under reduced pressure and a stream of helium at 90°C removed the target water. The tosylate (10 mg, 24 μmol), dissolved in dry acetonitrile (1.5 mL), was added to the dried [18F]F−/Kryptofix 222/K+ complex, and the vessel was heated for 8 min at 90°C. Afterward, the reaction mixture was loaded onto a silica Sep-Pak cartridge (Waters Corp., Milford, MA) and eluted with anhydrous ether. The solvents were removed by helium flow and heating. Two moles per liter hydrochloric acid (900 μL) were added to the dry residue, and the hydrolysis was performed at 90°C for 5 min. After cooling, 2N sodium hydroxide (800 μL) was added and the mixture was passed through a 0.45-μm polyvinylidene fluoride syringe filter (Waters) and injected onto a semipreparative high-performance liquid chromatography (HPLC) μBondapak C-18 column (7.8 × 300 mm, 10-μm packing; Waters). The column was

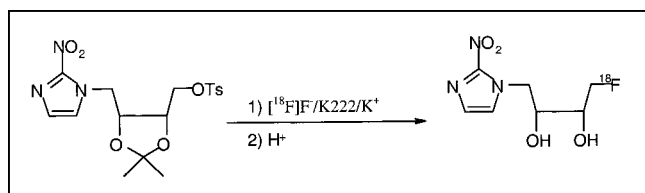eluted with saline (pH adjusted to 4.7 with hydrochloric acid) containing 2% ethanol (4 mL/min). The fraction containing [18F]FETNIM, eluting at 12–13 min, was collected. The hydrolyzed precursor eluted at 8–9 min. The radioactivity was measured, and the HPLC fraction was formulated for injection by being passed through a 0.22-μm sterile filter into a sterile injection bottle.

The final product was analyzed with HPLC. An aliquot was injected onto a μBondapak C-18 column (3.9 × 300 mm, 10-μm packing) eluted with water/acetonitrile (95/5 v/v) at a flow rate of 2 mL/min. The elution was monitored with an ultraviolet-absorption detector (λ = 215 nm) and a radioactivity detector. The retention time of authentic FETNIM was 4 min on this system. Radio–thin-layer chromatography (radio-TLC) was performed with silica gel 60 F_{254} plates (Merck) with chloroform/methanol (70/30 v/v) as the mobile phase. With this system, the R_f value of authentic FETNIM was 0.80.

Biodistribution of [18F]FETNIM in Rats

Twenty female Sprague-Dawley rats (Hsd:SD; mean body weight ± SD, 248 ± 15 g; Central Animal Laboratory, University of Turku, Turku, Finland) were studied for biodistribution of [18F]FETNIM. All animals bore multiple mammary tumors, which were induced in 50- ± 2-d-old female rats by single oral doses of 12 mg 7,12-dimethylbenz[a]anthracene (DMBA; Sigma, St. Louis, MO) in 1 mL sesame oil 6–8 wk before the study. Induction was performed in a special isolator (Metall & Plastic GmbH, Radolfzell, Germany) for 3 wk. The animals were housed under standard conditions (temperature, 21°C; humidity, 55% ± 5%; lights on from 6:00 AM to 6:00 PM) with free access to standard food and tap water. [18F]FETNIM doses of 8.5 ± 2.2 MBq (0.23 ± 0.06 mCi) for animals studied at 15, 30, and 60 min after injection and 50 ± 10 MBq (1.35 ± 0.27 mCi) for animals studied at 120 and 240 min were injected intravenously into a tail vein. The rats were killed in a carbon dioxide chamber 15 (n = 3), 30 (n = 3), 60 (n = 4), 120 (n = 7), or 240 (n = 3) min after the injection. Arterial blood was obtained through cardiac puncture, and multiple tissue samples were immediately obtained, counted for radioactivity in a well counter (7.62 × 7.62 cm [3 × 3 in.] NaI [Tl] crystal, 3MW3/3P; Bicron Inc., Newbury, OH), and weighed. Because DMBA induces multiple mammary tumors, the number of tumors sampled was higher than the number of animals. All data were corrected for background radioactivity and radioactivity decay. The amount of radioactivity was expressed as a percentage of injected dose per gram of tissue or blood (%ID/g).

Metabolism of [18F]FETNIM

Eighteen female Sprague-Dawley rats (Hsd:SD; mean body weight ± SD, 274 ± 26 g; Central Animal Laboratory, University of Turku) were studied for the metabolism of [18F]FETNIM. Eleven animals bore DMBA-induced tumors. A [18F]FETNIM dose of 55 ± 14 MBq (1.5 ± 0.4 mCi) was injected intravenously into a tail vein. The rats were killed in a carbon dioxide chamber 15 (n = 6), 30 (n = 3), 60 (n = 2), 120 (n = 4), or 240 (n = 3) min later. Arterial blood, liver, tumor, and, if obtained, urine samples were immediately removed, weighed, and counted for radioactivity as described above. Samples of the liver and tumor were homogenized in 0.9% sodium chloride/acetonitrile (95/5 v/v) with an automatic homogenizer (Polytron PT 3000; Kinematica, Littau, Switzerland) at 0°C.

Three dogs with spontaneous tumors (2 mammary carcinomas and 1 colon cancer) were imaged on an Advance PET scanner (General

FIGURE 1. Radiochemical synthesis of [18F]FETNIM from 1-(2′-nitro-1′-imidazolyl)-2,3-O-isopropylidene-4-tosyloxybutane.

Electric Medical Systems, Milwaukee, WI) after intravenous injection of a dose of 200 ± 5 MBq (5.4 ± 0.1 mCi) [^{18}F]FETNIM as a bolus. Blood samples were obtained from the dogs at 5 ($n = 3$), 15 ($n = 3$), 30 ($n = 3$), 60 ($n = 2$), and 90 ($n = 2$) min after injection.

Eight untreated patients with head and neck cancer were also imaged with the Advance PET scanner. A dose of 359 ± 16 MBq (9.7 ± 0.4 mCi) [^{18}F]FETNIM was injected intravenously as a bolus. The contralateral radial artery was cannulated for arterial blood sampling. Blood samples were taken 5, 10, 15, 20, 30, 40, 60, 80, 100, and 120 min after injection. An additional sample at 180 min was obtained from venous blood. The imaging data from the patients will be reported in a separate article.

Plasma was separated from whole blood in Vacutainer PST blood collection tubes (Becton, Dickinson and Co., Franklin Lakes, NJ) by centrifugation (10 min at room temperature, $1,100g$). Proteins from tissue homogenates, plasma, and urine were precipitated with acetonitrile, and the supernatants were used for radio-TLC analyses.

Protein binding of [^{18}F]FETNIM in plasma was determined by ultrafiltration using ultracentrifuge tubes (Mikrosep 30 K; Filtron Technology Corp., Northborough, MA) to separate plasma proteins (cutoff, 30,000 Da) from plasma. The amount of free [^{18}F]FETNIM was expressed as a percentage of the total radioactivity in the plasma.

Radio-TLC

Analysis of blood, urine, and tissue homogenates, as well as of [^{18}F]FETNIM standard solution, was performed by radio-TLC. Radio-TLC combined with digital autoradiography was preferred over radio-HPLC because of the vastly superior sensitivity of the combination and, in this case, equal chemical resolution with radio-HPLC. Sample solutions (2–30 μL) were applied on silica gel 60 F_{254} plates (Merck) as 8-mm bands by an automatic TLC sampler (ATS III; Camag, Muttenz, Switzerland). Standards were prepared by adding a small amount of [^{18}F]FETNIM to nonradioactive plasma just before the analysis. The standard samples were then handled using the same procedures as for regular samples. The plates were developed with a mixture of chloroform/methanol (70/30 v/v). After development, the plates were dried and radioactivity was detected by digital autoradiography (BAS 1800 analyzer and BAS-SR 2025 imaging plate; Fujifilm Co., Tokyo, Japan). The dynamic linear range of this system is 4 decades. The exposure time of the plate was 4 h.

RESULTS

Synthesis of [^{18}F]FETNIM

The decay-corrected synthesis yield of [^{18}F]FETNIM was 13%–20% ($n = 15$), as calculated from [^{18}F]F$^-$. The synthesis time was about 50 min. The radiochemical purity of [^{18}F]FETNIM at the end of synthesis exceeded 99%, and the product was found to be stable up to 4 h after the end of synthesis, as measured with radio-HPLC and radio-TLC. Ethanol was added to the eluent to avoid decomposition of the tracer. If no ethanol was used in the HPLC eluent, the radiochemical purity decreased with time—to about 85% in 8 h. The chemical purity of [^{18}F]FETNIM exceeded 95%, as measured with HPLC. The specific radioactivity of [^{18}F]FETNIM was about 330 GBq/μmol (decay corrected to the end of cyclotron bombardment).

Biodistribution of [^{18}F]FETNIM

The biodistribution of [^{18}F]FETNIM in rats with DMBA tumors at various times is shown in Table 1. The highest uptakes at 120 min were observed in urine and kidney. In accordance with the low lipophilicity of the tracer, the lowest uptake was seen in fat and cerebellum. The tumor-to-blood radioactivity ratio reached a maximum at 120 min and remained constant thereafter until 240 min (Table 2). The tumor-to-muscle ratio was also constant during the same period.

Metabolism of [^{18}F]FETNIM

The amount of unchanged [^{18}F]FETNIM at different times in rat plasma, liver, and tumor homogenates is shown in Table 3. Examples of typical radio-TLC chromatograms from human arterial plasma and rat liver and tumor are shown in Figure 2. Plasma samples were also analyzed from dogs and patients at different times during PET imaging. In rat arterial plasma, most radioactivity was recovered as unchanged tracer, whereas the liver showed almost no native [^{18}F]FETNIM. In tumor, the average fraction of unchanged tracer was about 20% during the first 120 min and declined to 10% by 240 min (Table 3). Radiolabeled metabolites in liver were seen at R_f values of 0.03 and 0.21. Radio-TLC analyses showed that the value of unchanged [^{18}F]FETNIM in dog venous plasma ($n = 3$) was constant at 86% $\pm$ 4% over the 90-min dynamic scan. The average amount of [^{18}F]FETNIM in human arterial plasma was constant at 92% $\pm$ 5% over the 180-min scan. The major metabolic product detected in plasma was seen at an R_f value of 0.03. A minor metabolite was also detected at an R_f value of 0.64 in blood samples between 5 and 30 min.

Urine samples were also analyzed from all species. The amount of unchanged [^{18}F]FETNIM in rat urine was 83% $\pm$ 2% at 15 ($n = 1$), 20 ($n = 1$), and 240 ($n = 1$) min after injection. Urine from a dog was collected on only 1 occasion. At 90 min after the injection of [^{18}F]FETNIM, the amount of unchanged tracer in this single sample of dog urine was 84%. In human urine, the amount of unchanged [^{18}F]FETNIM was 73% $\pm$ 21% ($n = 7$; range, 21%–96%) 140 min after injection. The only metabolite detected in urine was seen at an R_f value of 0.03.

Protein Binding of [^{18}F]FETNIM in Plasma

Binding of [^{18}F]FETNIM to plasma proteins was invariably low in all species. The binding also showed little intersubject variation and was stable up to 240 min after injection, when the last blood samples were collected. The average amount of unbound [^{18}F]FETNIM was 98% $\pm$ 5% in rats (15–240 min), 95% $\pm$ 2% in patients (5–180 min), and 96% $\pm$ 5% in dogs (5–90 min).

DISCUSSION

In the current study, [^{18}F]FETNIM was produced at a moderate radiochemical yield. Raising the reaction temperature and prolonging the reaction time did not improve

TABLE 1
Biodistribution of [¹⁸F]FETNIM in Rats Bearing DMBA-Induced Mammary Tumors

Tissue	15 min (n = 3)	30 min (n = 3)	60 min (n = 4)	120 min (n = 7)	240 min (n = 3)
Blood	0.325 ± 0.056	0.333 ± 0.056	0.206 ± 0.004	0.099 ± 0.024	0.053 ± 0.009
Plasma	0.313 ± 0.064	0.310 ± 0.047	0.155 ± 0.015*	0.080 ± 0.003†	0.030 ± 0.007
Heart	0.338 ± 0.084	0.359 ± 0.057	0.246 ± 0.011	0.134 ± 0.032	0.071 ± 0.010
Lung	0.357 ± 0.056	0.360 ± 0.053	0.246 ± 0.014	0.113 ± 0.028	0.057 ± 0.008
Liver	0.400 ± 0.100	0.478 ± 0.091	0.322 ± 0.011	0.168 ± 0.046	0.142 ± 0.043
Spleen	0.329 ± 0.088	0.338 ± 0.061	0.213 ± 0.007	0.102 ± 0.023	0.054 ± 0.010
Kidney	0.737 ± 0.069	1.200 ± 0.450	0.504 ± 0.024	0.397 ± 0.092	0.231 ± 0.041
Bladder	2.10 ± 1.70	1.67 ± 0.89	0.90 ± 0.29	0.73 ± 0.71	NA
Urine	35 ± 11‡	NA	NA	14 ± 5§	18 ± 9
Adrenal gland	0.379 ± 0.074	0.480 ± 0.130	0.386 ± 0.094	0.177 ± 0.054	0.080 ± 0.002
Pancreas	0.246 ± 0.097	0.336 ± 0.059	0.186 ± 0.015	0.103 ± 0.022	0.063 ± 0.012
Intestine	0.330 ± 0.110	0.370 ± 0.065	0.360 ± 0.100	0.230 ± 0.150	0.129 ± 0.018
Stomach	0.320 ± 0.130	0.328 ± 0.038	0.370 ± 0.180	0.146 ± 0.036	NA
Fat (subcutaneous)	0.045 ± 0.012	0.043 ± 0.015	0.035 ± 0.010	0.013 ± 0.004	0.010 ± 0.006
Muscle	0.263 ± 0.065	0.345 ± 0.048	0.242 ± 0.009	0.116 ± 0.023	0.061 ± 0.011
Ovary	0.400 ± 0.120	0.418 ± 0.085	0.255 ± 0.023	0.123 ± 0.021	NA
Bone (skull)	0.054 ± 0.016	0.071 ± 0.009	0.058 ± 0.007	0.087 ± 0.052	0.025 ± 0.003
Marrow	0.480 ± 0.150	0.630 ± 0.270	0.372 ± 0.067	0.119 ± 0.038	NA
Cerebellum	0.069 ± 0.029	0.103 ± 0.024	0.094 ± 0.016	0.063 ± 0.009	0.045 ± 0.004
Tumor	0.480 ± 0.10*	0.383 ± 0.096‡	0.239 ± 0.037§	0.178 ± 0.046‖	0.087 ± 0.043¶

*n = 2.
†n = 3.
‡n = 5.
§n = 6.
‖n = 23.
¶n = 21.
NA = not available.
Data are mean ± SD %ID/g.

radiochemical yields. Several chemical impurities were generated in the synthesis, of which hydrolysis products of unreacted precursor were of particular concern. All impurities were, however, efficiently removed by semipreparative HPLC purification.

The overall biodistribution of [¹⁸F]FETNIM in rat tissues was uniform and generally consistent with that reported for previously studied nitroimidazoles (8,12,14,15), except for some organs. Notably, the cerebellum and subcutaneous fat had a low uptake (Table 1), which is explained by the low lipophilicity of [¹⁸F]FETNIM compared with misonidazole and [¹⁸F]FMISO (12). The tracer also showed a much lower liver uptake (1.68 ± 0.62 liver-to-blood ratio) than that

reported by Rasey et al. (8) for [¹⁸F]FMISO (6.67 ± 0.95 liver-to-blood ratio) at 2 h after injection. High liver uptake has also been reported for other nitroimidazole compounds, such as [¹⁸F]fluoroetanidazole (14), 1-(3-[¹⁸F]fluoropropyl)-2-nitroimidazole (13), and some other ¹⁸F-labeled fluoronitroimidazole analogs (11). Our biodistribution studies showed that urine and kidney had the highest uptake (Table 1). These results agree with earlier findings by Yang et al. (12) and indicate that [¹⁸F]FETNIM is less metabolized in the liver and more actively excreted through the renal pathway than are other, more lipophilic nitroimidazole compounds suggested for imaging of hypoxia thus far. According to metabolite studies using radio-TLC, about 98% of the

TABLE 2
Ratios of [¹⁸F]FETNIM in Rats Bearing DMBA-Induced Mammary Tumors

Ratio	15 min (n = 3)	30 min (n = 3)	60 min (n = 4)	120 min (n = 7)	240 min (n = 3)
Tumor-to-blood	1.49 ± 0.40	1.15 ± 0.35	1.16 ± 0.18	1.79 ± 0.64	1.65 ± 0.87
Liver-to-blood	1.23 ± 0.37	1.44 ± 0.37	1.56 ± 0.06	1.69 ± 0.62	2.70 ± 0.94
Muscle-to-blood	0.81 ± 0.24	1.04 ± 0.23	1.17 ± 0.05	1.17 ± 0.37	1.16 ± 0.30
Tumor-to-muscle	1.84 ± 0.59	1.11 ± 0.32	0.99 ± 0.16	1.53 ± 0.50	1.42 ± 0.76

Data are mean ± SD.

TABLE 3
Percentage of Unchanged [¹⁸F]FETNIM in Rat Tissues

Time (min)	Plasma %	n	Liver %	n	Tumor %	n
15	72 (66–78)	6	5.0	1	16	1
30	87 (85–88)	3	1.5 (0.6–2.3)	3	21 (3–45)	4
60	84 (83–86)	2	1.5 (0.6–2.3)	2	24 (9–49)	3
120	80 (77–84)	3	0.2 (0.0–1.0)	4	23 (6–71)	5
240	71 (69–74)	2	1.4 (0.0–2.3)	3	10 (5–14)	6

Data are mean (range).

radioactivity recovered from rat liver was associated with unidentified metabolites (Table 3). The liver-to-blood activity ratio showed an increase as a function of time (Table 2).

Bone uptake was measured to monitor whether defluorination of the tracer occurred. As shown in Table 1, we observed only minimal defluorination, and the bone (skull) uptake we measured (0.058 ± 0.007 %ID/g tissue) was much lower than that previously reported by Yang et al. (*12*) (0.26 ± 0.14 %ID/g tissue) at 1 h after injection. On the other hand, we measured high uptake in the bone marrow (0.37 ± 0.07 %ID/g tissue), suggesting that at least a part of

the high bone activity detected by Yang et al. was recovered from marrow rather than organic bone matrix. The lung uptake was low, as it should be in well-oxygenated organs; the lung-to-blood ratio was 1.14 ± 0.40 at 2 h. However, high uptake was measured in the intestine, possibly because of excretion of radioactive metabolites of [¹⁸F]FETNIM by the liver through enterohepatic circulation. Rasey et al. (*23*) also reported high ³H uptake of [³H]FMISO in the gut of KHT tumor–bearing mice.

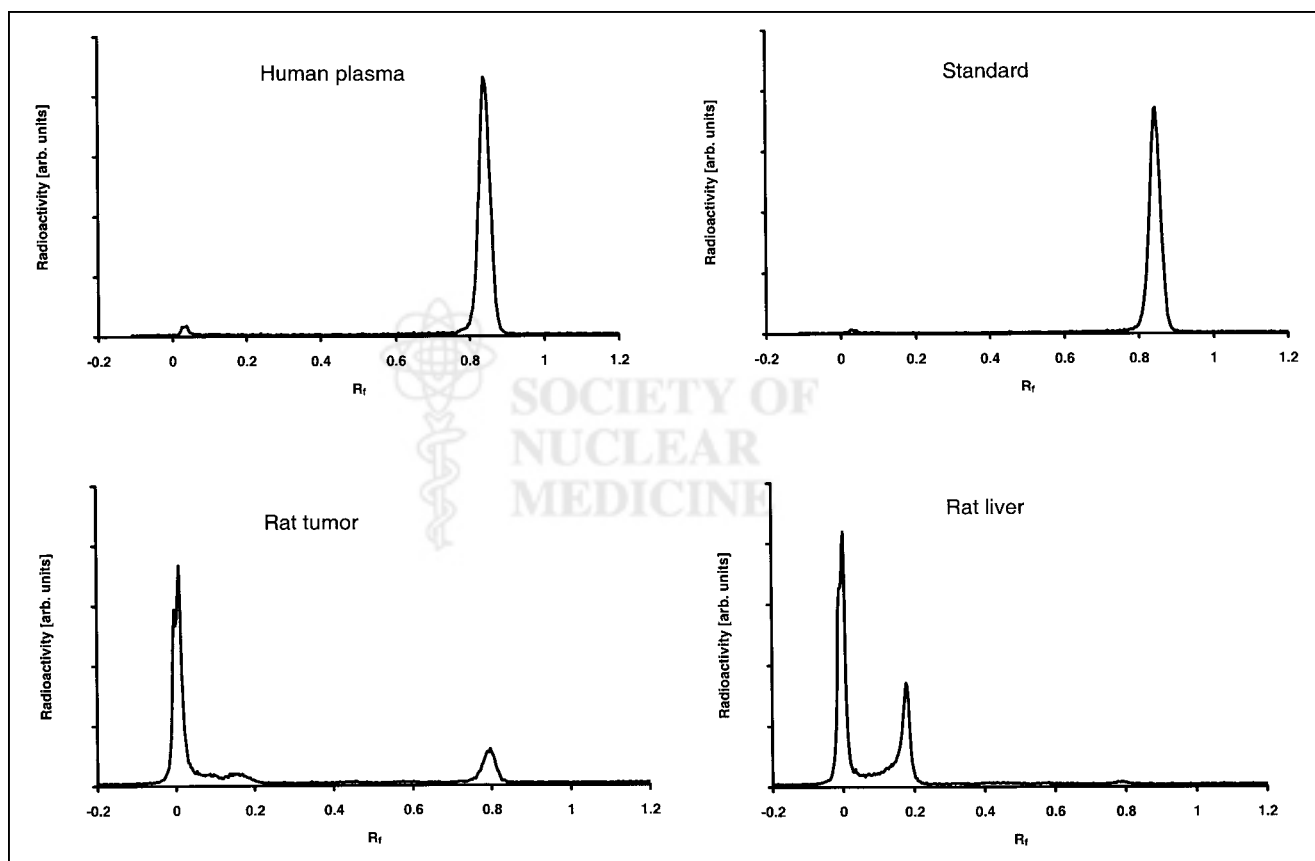Moderate uptake could be detected in DMBA-induced rat mammary tumors. The highest tumor-to-blood ratio ($1.80 \pm$

FIGURE 2. Typical chromatograms of rat and human tissues as detected by radio-TLC and digital autoradiography. Human plasma sample was analyzed at 30 min after injection of [¹⁸F]FETNIM, whereas rat tumor and liver samples were analyzed at 60 min. Radiochromatograms of rat and human plasma were qualitatively and quantitatively similar. arb. = arbitrary.
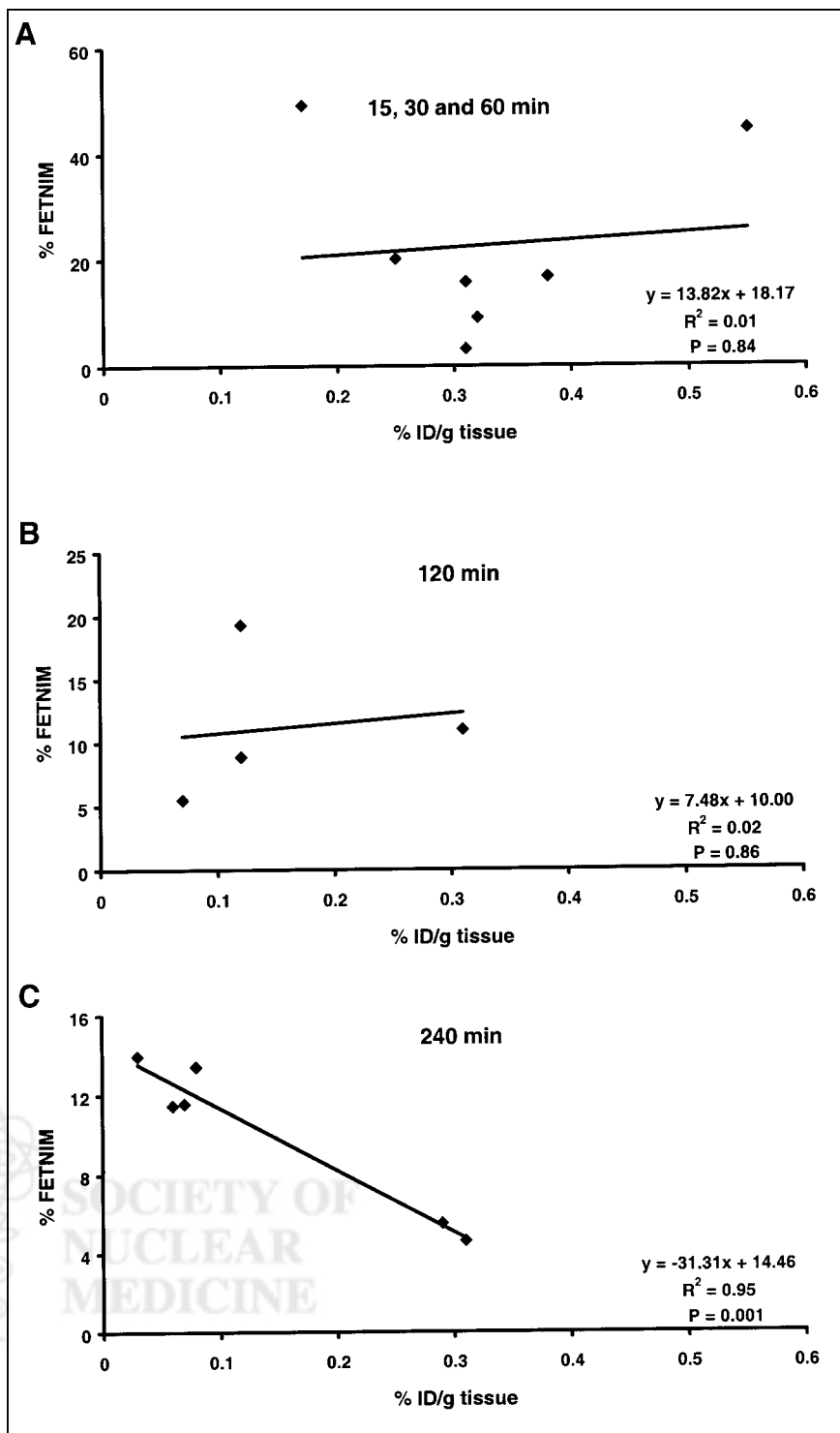
FIGURE 3. Relationship between percentage of unchanged [18F]FETNIM and uptake in DMBA-induced rat tumors. Poor correlation was observed at early times (A and B), but, at later time, significant inverse correlation was found (C).

0.64) was measured at 2 h after injection, and at 4 h the ratio was comparable, at 1.64 ± 0.87. Chung et al. (24) also reported a tumor-to-blood ratio of about 1.5 in a murine sarcoma model at 2 h after injection, as studied with [18F]FETNIM. The tumor uptake we measured was notably lower than that observed in the model (DMBA-induced tumor cell line) used by Yang et al. (12). They reported a tumor-to-blood ratio of 2.4 at 2 h after injection of

[18F]FETNIM, and this ratio increased to 8.0 at 4 h. This rather large difference in the tumor-to-blood ratios was probably caused by the different tumor models. The DMBA-induced tumor mimics human hormone-dependent breast cancer and might retain more natural characteristics than do tumors established from cell lines with known (and high) hypoxic fractions. Oxygenation is known to be heterogeneous at the microregional level within the tumor, and

great variability in the proportion of hypoxic cells has been found between different types of experimental and human tumors (*10,25,26*). Tumor uptake, expressed as %ID/g tissue, does not necessarily depict the local radioactivity distribution within the whole tumor mass, even if this term is suitable in the case of homogeneous tissues. The tumor-to-blood ratio of [^{18}F]FETNIM that we measured at 2 h after injection (1.80 ± 0.64) is more similar to the earlier reported values for [^{18}F]FMISO, with a tumor-to-blood uptake ratio of about 2 detected in mice (*23*), rats (*27*), and humans (*9*) 2–4 h after injection. In comparison with these earlier reported values, the tumor-to-blood uptake ratio for [^{18}F]FMISO reported by Yang et al. was significantly higher (2.24 ± 0.20 and 3.78 ± 0.68 at 2 and 4 h, respectively) after injection. Their findings may have been caused by exceptionally high reductase activity or the hypoxic fraction of the tumor model they used.

Tumor tissues were also analyzed for the presence of labeled metabolites. Consistent with the presumed heterogeneity of our tumor model, we found a variation of 3%–70% in the proportion of unchanged [^{18}F]FETNIM in the tumor. An inverse correlation was present between the percentage of unchanged [^{18}F]FETNIM and regional tumor uptake (%ID/g) as a function of time (Fig. 3). The best correlation (r^2 = 0.94; P = 0.001) was seen at 4 h after injection. These data indicate that a high radioactivity concentration in the tumor is inversely correlated with the fraction of native [^{18}F]FETNIM in tumor tissue after allowing sufficient time for metabolic conversion. This correlation is in agreement with the assumption that nitroimidazole compounds are metabolically trapped in tissues with low oxygen tensions (*28*).

The amount of unchanged [^{18}F]FETNIM in plasma remained constant over time, although a slight variation of between 80% and 90% was seen in all species. The radioactivity in the urine samples from the humans and 1 dog also contained mostly unchanged tracer, although some variation between patients was seen. [^{18}F]FETNIM did not show binding to plasma proteins in the species investigated. Protein binding of <20% has been reported for nitroimidazoles such as metronidazole (*29*), tinidazole (*30*), and ornidazole (*31*). Misonidazole does not seem to bind to proteins (*32*).

CONCLUSION

We showed, in 3 species, that a major fraction of radioactivity recovered from plasma represents unchanged [^{18}F]FETNIM, whereas extensive and rapid metabolism of [^{18}F]FETNIM in the liver leads to the appearance of 2 major labeled metabolites. High excretion of unchanged [^{18}F]FETNIM in urine was seen in all species, whereas a low concentration of radioactivity was detected in rat cerebellum and subcutaneous fat. These findings are consistent with low lipophilicity and rapid clearance of tracer from tissue compartments with low metabolism of [^{18}F]FETNIM.

The small fraction of metabolites of [^{18}F]FETNIM in plasma and urine, as well as the low protein binding, indicates that no metabolite corrections for input are necessary for dynamic [^{18}F]FETNIM PET imaging. Further, our data suggest that [^{18}F]FETNIM shows increasing metabolic retention in DMBA rat tumor as a function of time. The metabolic retention probably represents cellular binding of [^{18}F]FETNIM adducts in macromolecular fractions and may thus indicate regions of low oxygen concentration within the tumor. Therefore, this tracer may have a potential use in PET studies on hypoxia of cancer patients.

REFERENCES

1. Gray LH, Conger AD, Ebert M, Hornsey S, Scott OCA. Concentration of oxygen dissolved in tissues at the time of irradiation as a factor in radiotherapy. *Br J Radiol.* 1953;26:638–648.
2. Graeber TG, Osmanian C, Jacks T, et al. Hypoxia-mediated selection of cells with diminished apoptotic potential in solid tumours. *Nature.* 1996;379:88–91.
3. Höckel M, Schlenger K, Aral B, Mitze M, Schäffer U, Vaupel P. Association between tumor hypoxia and malignant progression in advanced cancer of the uterine cervix. *Cancer Res.* 1996;56:4509–4515.
4. Wang GL, Semenza GL. Characterization of hypoxia-inducible factor 1 and regulation of DNA binding activity by hypoxia. *J Biol Chem.* 1993;268:21513–21518.
5. Raleigh JA, Dewhirst MW, Thrall DE. Measuring tumor hypoxia. *Semin Radiat Oncol.* 1996;6:37–45.
6. Chapman JD. Hypoxic sensitizers: implications for radiation therapy. *N Engl J Med.* 1979;301:1429–1432.
7. Parliament M, Urtasun R. Misonidazole labeling as a marker of cellular hypoxia. In: Molls M, Vaupel P, eds. *Blood Perfusion and Microenvironment of Human Tumors.* New York, NY: Springer; 1998:89–99.
8. Rasey JS, Grunbaum Z, Magee S, et al. Characterization of radiolabeled fluoromisonidazole as a probe for hypoxic cells. *Radiat Res.* 1987;111:292–304.
9. Koh WJ, Rasey JS, Evans ML, et al. Imaging of hypoxia in human tumors with [F-18]fluoromisonidazole. *Int J Radiat Oncol Biol Phys.* 1991;22:199–212.
10. Rasey JS, Koh WJ, Evans ML, et al. Quantifying regional hypoxia in human tumors with positron emission tomography of [^{18}F]fluoromisonidazole: a pretherapy study of 37 patients. *Int J Radiat Oncol Biol Phys.* 1996;36:417–428.
11. Jerabek PA, Patrick TB, Kilbourn MR, Dischino DD, Welch MJ. Synthesis and biodistribution of ^{18}F-labeled fluoronitroimidazoles: potential *in vivo* markers of hypoxic tissue. *Int J Radiat Appl Instrum [A].* 1986;37:599–605.
12. Yang DJ, Wallace S, Cherif A, et al. Development of F-18-labeled fluoroerythronitroimidazole as a PET agent for imaging tumor hypoxia. *Radiology.* 1995; 194:795–800.
13. Yamamoto F, Oka H, Antoku S, Ichiya Y, Masuda K, Maeda M. Synthesis and characterization of lipophilic 1-[^{18}F]fluoroalkyl-2-nitroimidazoles for imaging hypoxia. *Biol Pharm Bull.* 1999;22:590–597.
14. Rasey JS, Hofstrand PD, Chin LK, Tewson TJ. Characterization of [^{18}F]fluoroetanidazole, a new radiopharmaceutical for detecting tumor hypoxia. *J Nucl Med.* 1999;40:1072–1079.
15. Evans SM, Kachur AV, Shiue CY, et al. Noninvasive detection of tumor hypoxia using the 2-nitroimidazole [^{18}F]EF1. *J Nucl Med.* 2000;41:327–336.
16. Lewis JS, McCarthy DW, McCarthy TJ, Fujibayashi Y, Welch MJ. Evaluation of ^{64}Cu-ATSM in vitro and in vivo in a hypoxic tumor model. *J Nucl Med.* 1999;40:177–183.
17. Mannan RH, Somayaji VV, Lee J, Mercer JR, Chapman JD, Wiebe LI. Radio-iodinated 1-(5-iodo-5-deoxy-β-D-arabinofuranosyl)-2-nitroimidazole (iodoazo-

mycin arabinoside: IAZA): a novel marker of tissue hypoxia. *J Nucl Med.* 1991;32:1764–1770.

18. Groshar D, McEvan AJ, Parliament MB, et al. Imaging tumor hypoxia and tumor perfusion. *J Nucl Med.* 1993;34:885–888.

19. Stypinski D, Wiebe LI, McEvan AJ, Schmidt RP, Tam YK, Mercer JR. Clinical pharmacokinetics of ^{123}I-IAZA in healthy volunteers. *Nucl Med Commun.* 1999; 20:559–567.

20. Ballinger JR, Kee JWM, Rauth AM. In vitro and in vivo evaluation of a technetium-99m-labeled 2-nitroimidazole (BMS181321) as a marker of tumor hypoxia. *J Nucl Med.* 1996;37:1023–1031.

21. Yutani K, Kusuoka H, Fukuchi K, Tatsumi M, Nishimura T. Applicability of ^{99m}Tc-HL91, a putative hypoxic tracer, to detection of tumor hypoxia. *J Nucl Med.* 1999;40:854–861.

22. Melo T, Duncan J, Ballinger JR, Rauth AM. BRU59-21, a second-generation ^{99m}Tc-labeled 2-nitroimidazole for imaging hypoxia in tumors. *J Nucl Med.* 2000;41:169–176.

23. Rasey JS, Koh WJ, Grierson JR, Grunbaum Z, Krohn KA. Radiolabeled fluoromisonidazole as an imaging agent for tumor hypoxia. *Int J Radiat Oncol Biol Phys.* 1989;17:985–991.

24. Chung JK, Chang YS, Lee YJ, et al. The effect of tumor size on F-18-labeled fluorodeoxyglucose and fluoroerythronitroimidazole uptake in a murine sarcoma model. *Ann Nucl Med.* 1999,13:303–308.

25. Moulder JE, Rockwell S. Hypoxic fractions of solid tumors: experimental techniques, methods of analysis, and a survey of existing data. *Int J Radiat Oncol Biol Phys.* 1984;10:695–712.

26. Vaupel P, Kallinowski F, Okunieff P. Blood flow, oxygen and nutrient supply, and metabolic microenvironment of human tumors: a review. *Cancer Res.* 1989; 49:6449–6465.

27. Kubota K, Tada M, Yamada S, et al. Comparison of the distribution of fluorine-18 fluoromisonidazole, deoxyglucose and methionine in tumour tissue. *Eur J Nucl Med.* 1999;26:750–757.

28. Edwards DI. Nitroimidazole drugs: action and resistance mechanisms. 1. Mechanisms of action. *J Antimicrob Chemother.* 1993;31:9–20.

29. Sanvordeker DR, Chien YW, Lin TK, Lambert HJ. Binding of metronidazole and its derivatives to plasma proteins: an assessment of drug binding phenomenon. *J Pharm Sci.* 1975;64:1797–1803.

30. Taylor JA Jr, Migliardi JR, Von Wittenau MS. Tinidazole and metronidazole pharmocokinetics in man and mouse. *Antimicrob Agents Chemother.* 1969;9: 267–270.

31. Schwarz DE, Jeunet F. Comparative pharmacokinetic studies of ornidazole and metronidazole in man. *Chemotherapy.* 1976;22:19–29.

32. Workman P. Pharmacokinetics of hypoxic cell radiosensitizers. *Cancer Clin Trials.* 1980;3:237–251.